

Quantum criticality near the Stoner transition in a two-dot with spin-orbit coupling

Oleksandr Zelyak* and Ganpathy Murthy†

*Department of Physics and Astronomy,
University of Kentucky, Lexington, Kentucky 40506, USA*

(Dated: June 30, 2022)

Abstract

We study a system of two tunnel-coupled quantum dots, with the first dot containing interacting electrons (described by the Universal Hamiltonian) not subject to spin-orbit coupling, whereas the second contains non-interacting electrons subject to spin-orbit coupling. We focus on describing the behavior of the system near the Stoner transition. Close to the critical point quantum fluctuations become important and the system enters a quantum critical regime. The large- N approximation allows us to calculate physical quantities reliably even in this strongly fluctuating regime. In particular, we find a scaling function to describe the crossover of the quasiparticle decay rate between the renormalized Fermi liquid regime and the quantum critical regime.

PACS numbers: **73.21.La**, **05.40.-a**, **73.50.Jt**

Keywords: quantum dot, scaling function, crossover, quantum criticality, Stoner instability

arXiv:0906.1838v1 [cond-mat.mes-hall] 9 Jun 2009

I. INTRODUCTION

The transport of electrons through mesoscopic systems at low temperatures is a coherent process. The manifestations of coherent electronic motion are weak localization, Aharonov-Bohm oscillations, persistent current, etc.¹

Though many mesoscopic effects can be explained in the framework of non-interacting electrons, there is a vast amount of evidence showing that collective effects of the electron spin are important in predicting the behavior of the system. Apart from its fundamental interest, studying interaction-related effects on the electronic spin is important from a technological point of view.

The spin of the electron couples to the external magnetic field and to the orbital degrees of freedom. This spin-orbit coupling (SO) is caused by a non-zero electric field in the laboratory reference frame that is transformed into a magnetic field in the electron's rest frame. In bulk systems the SO coupling results from the absence of inversion symmetry in the crystalline lattice² (Dresselhaus term). In finite size systems, such as metallic grains or semiconductor quantum dots, an additional contribution to SO coupling comes from the structure inversion asymmetry³ (Rashba term), the simplest example of which is a two-dimensional electron gas (2DEG) confined to an interface, in which the confining electric field perpendicular to the 2DEG is the source of the SO coupling.

In diffusive and ballistic/chaotic mesoscopic systems the kinetic term in the full Hamiltonian is well described by Random Matrix Theory^{4,5} (RMT). RMT has been very successful in describing the ensemble averages of one-particle spectral correlations as well as correlations of eigenfunctions.

RMT describes the universal zero-dimensional limit in a mesoscopic system. Its regime of validity is when all time scales (the spin-orbit relaxation time τ_{SO} and the inverse mean level spacing δ^{-1}) are much larger than ergodic time $\tau_{erg} = \hbar/E_T$. Alternatively, all relevant energy scales should be smaller than Thouless energy E_T (for a diffusive dot of linear scale L , $E_T \simeq \hbar D/L^2$, where D is the diffusion constant, while for a ballistic/chaotic dot $E_T \simeq \hbar v_F/L$).

Even though $\tau_{SO} \gg \tau_{erg}$ defines the universal limit, to decide if the SO coupling is important for a particular physical process, τ_{SO} should be compared to other characteristic time scales.^{6,7,8} As the SO coupling is increased from zero in a noninteracting system, its

effects begin to become important for physical quantities when the inverse SO relaxation time is comparable to the mean level spacing $\delta \sim \tau_{SO}^{-1}$. In interacting systems near a degeneracy point between two ground states of different spin, even much tinier SO couplings can have order one effects.⁹

RMT systems can be classified according to the presence or absence of time reversal (TR) and spin rotation symmetries. They fall into three major categories described by the “classical” RMT ensembles introduced by Dyson. The systems with both symmetries preserved belong to the Gaussian Orthogonal ensemble. Systems with broken TR symmetry (e.g. by an external magnetic field) are described by the Gaussian Unitary ensemble. Finally, systems with TR preserved and broken spin rotation symmetry belong to the Gaussian Symplectic ensemble.

In the universal regime, the SO coupling has significant effect on spectral properties of eigenvalues and eigenfunctions. One can relate the spin-orbit scattering length L_{SO} to a SO crossover energy scale $E_X = E_T \left(\frac{L}{L_{SO}}\right)^2$. For energies below E_X , the one-particle term in the Universal Hamiltonian is modeled by a Gaussian symplectic random matrix. If one wants to describe energies both above and below E_X , one has to use the RMT ensemble which is in a crossover between the GOE and the GSE classes.^{4,10}

The interactions in mesoscopic systems at low temperatures are described by the Universal Hamiltonian:^{11,12,13,14}

$$H_U = \sum_{\alpha,s} \epsilon_\alpha c_{\alpha,s}^\dagger c_{\alpha,s} + \frac{U_0}{2} \hat{N}^2 - J \mathbf{S}^2 + \lambda T^\dagger T, \quad (1)$$

where \hat{N} is the total particle number, \mathbf{S} is the total spin, and $T = \sum c_{\beta,\downarrow} c_{\beta,\uparrow}$. The Universal Hamiltonian contains a charging energy U (direct channel), a Stoner exchange energy J (spin channel) and a reduced superconducting interaction λ (Cooper channel). A renormalization group (RG) analysis reveals^{15,16} that this is the low-energy effective theory for weak coupling, although other effective theories and other ground states can be accessed for strong coupling.¹⁷

For small normal metallic grains and non-superconducting quantum dots with a fixed number of particles the exchange interaction is the main contribution to electron-electron interactions. The short range part of electron-electron interactions causes the ferromagnetic Stoner instability at large values of exchange energy J .

In the absence of SO coupling the total spin of the system \mathbf{S}^2 and its z-projection S_z commute with kinetic energy term and are good quantum numbers. Typically for metallic grains the exchange constant $J \lesssim \delta$.

For weak exchange interaction $J \ll \delta$ the spin of the ground state for odd number of electrons is $1/2$. As J gets larger, there is a non-zero probability to obtain a ground state with $S > 1/2$. This happens when the cost in orbital energy to promote an electron to the next level is less than the energy gain due to the exchange interaction. As J approaches δ , the total spin of the system grows¹⁴, and at $J = \delta$ the system undergoes a phase transition (the Stoner transition) into a "bulk" ferromagnetic state. For $J \geq \delta$ the magnetization of the system is proportional to the number of electrons N .

In the presence of SO coupling the total spin does not commute with full Hamiltonian $[H, \mathbf{S}^2] \neq 0$. While the dominant effect of the electron-electron interaction is to organize the states according to total spin \mathbf{S} , the SO term produces matrix elements between states of different spin, which randomizes spin, and also leads to sample-to-sample fluctuations of the matrix elements of the electron-electron interaction¹⁰ and the suppression of the exchange interaction.^{7,18}

When $J \gg \gamma_{SO}$, the SO coupling is simply ignored (unless one is near a degeneracy between ground states of different spin.⁹) In the opposite limit $J \ll \delta$ and $J \ll \gamma_{SO}$ electron-electron interactions are suppressed and expectation value of total spin in ground state $\langle S \rangle < 1/2$. The interesting regime is when $\gamma_{SO} \sim J \lesssim \delta$. In this case the exchange interaction is not completely suppressed, and the fluctuations of total spin are comparable to its expectation value. This regime is driven by the combined effect of spin-orbit scattering and electron-electron interactions.

We study the regime where the system is near the Stoner instability $J \rightarrow \delta^-$. If SO coupling is absent, there are no quantum fluctuations of the spin, and one obtains a sequence of metamagnetic transitions with the true Stoner transition being the accumulation point.¹⁴ In the presence of SO coupling, at low energies, the behavior of the system is dominated by quantum critical fluctuations leading to the formation of a quantum critical regime (QCR).^{19,20}

Imagine that one is at some $J < \delta$, but that $1 - J/\delta \ll 1$. Even close to the transition one can think of two different regimes of energy separated by a many-body crossover scale E_{QCX} , which will turn out to be simply related to the single-particle RMT crossover scale E_X .¹⁹ For

$\omega \ll E_{QCX}$ the system behaves as though it were a renormalized Fermi liquid, with altered Fermi liquid parameters and a quasiparticle decay rate going as ω^2 .^{21,22} On the other hand, for $E_{QCX} \lesssim \omega$, the behavior is controlled by the quantum critical point. The change of behavior as one increases ω is described by a universal scaling function $F(\omega/E_{QCX})$.

The critical point and QCR are dominated by many-body quantum fluctuations, and thus the scaling functions cannot be calculated perturbatively. However, it turns out that as long as $E_{QCX}, \omega \gg \delta$, one can use a large- N approximation with $\min(\frac{E_{QCX}}{\delta}, \frac{\omega}{\delta})$ playing the role of the large N .¹⁹ This allows us to compute the scaling functions reliably.

From the point of view of experiment, the key point is that one can control E_{QCX} , which is a many-body scale, by tuning a single-particle crossover energy scale E_X . Thus, at a fixed value of the parameter J , one can tune oneself into and out of the QCR by tuning a single-particle knob.

As a prerequisite to describing the system near Stoner transition, we consider the non-interacting case and calculate ensemble-averaged one and two particle Green's functions for electrons in the first dot coupled to the second dot in crossover between GOE and GSE ensembles. The one particle Green's function is unchanged by crossover, though it is modified by interdot coupling. The two particle Green's function is the sum of the contributions due to diffuson²³ mode and Cooperon modes. Both contributions depend on the ratios of crossover parameter E_{X_2} , interdot coupling parameter E_U , and measurement energy ω .

It may seem counterintuitive that one can use *non-interacting* wavefunction averages to describe the behavior of a system with strong many-body fluctuations^{10,18,19,24}, but this goes hand in hand with the use of the large- N approximation. This is because there is no wavefunction renormalization to leading order in the the large- N approximation.

II. MODEL DEFINITION

We consider a system of two quantum dots (metallic grains) coupled to each other by tunneling (see Fig. 1). The motion of electrons can be either diffusive or ballistic/chaotic: in either case the single-particle energies and wavefunctions are controlled by RMT, which is all that we require.

For the non-interacting system the ensemble-averaged spectral and eigenvector correlations can be computed by RMT.^{4,5} The first dot belongs to the GOE, since it has no

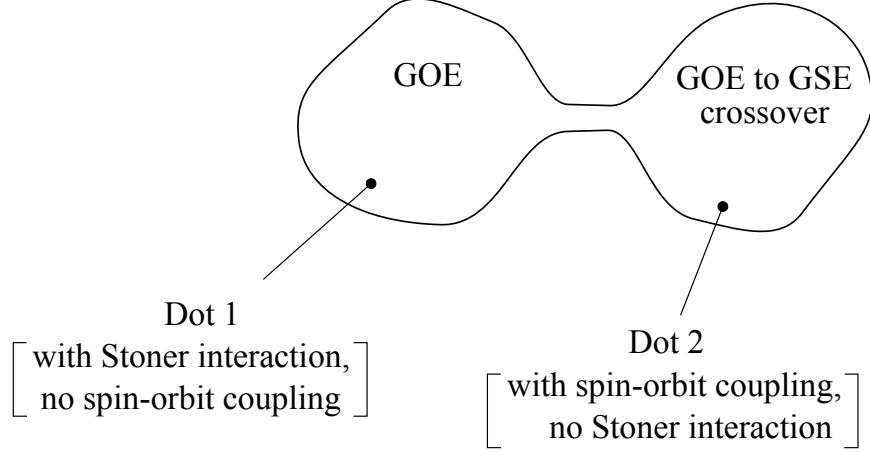


FIG. 1: Two coupled quantum dots in GOE-to-GSE crossover.

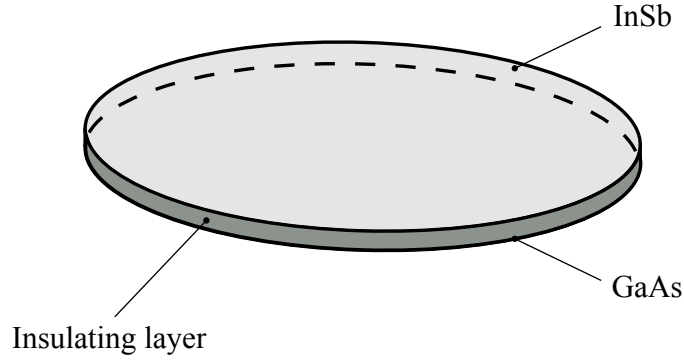


FIG. 2: (Color online) The vertical arrangement of the dots allows us to get rid of the charging energy.

spin-orbit coupling. The second dot has weak spin orbit coupling that drives it into the GOE→GSE crossover, characterized by a crossover scale E_{X_2} . We also assume that there is a Stoner exchange interaction in the first dot. No interactions are present in the second dot. The tunneling between the dots gives rise to another crossover scale E_U , where E_U/δ is the dimensionless conductance between the two dots.

In Fig. 2 one can see a more realistic picture of the system. In an experimental setup the lower dot could be made of *GaAs* (with significant exchange interaction but tiny SO coupling), while the upper dot could be made of *InSb* (with large spin-orbit coupling). The choice of the vertically coupled geometry will be discussed below.

In the low-energy limit interactions are described by Universal Hamiltonian.^{11,12,13,14} (1) For our system H_U has the form:

$$\begin{aligned}
H &= \sum_{i_0 j_0 s} H_{i_0 j_0}^{(1)} c_{i_0, s}^\dagger c_{j_0, s} - JS^2 + \sum_{\mu_0 \nu_0 s} H_{\mu_0 \nu_0}^{(2)} c_{\mu_0, s}^\dagger c_{\nu_0, s} + \sum_{i_0 \mu_0 s} V_{i_0 \mu_0} (c_{i_0, s}^\dagger c_{\mu_0, s} + H.c) \\
&= \sum_{\mu \tau} \epsilon_\mu c_{\mu, \tau}^\dagger c_{\mu, \tau} - JS^2,
\end{aligned} \tag{2}$$

where $H^{(2)}$ contains the effect of spin orbit coupling in the second dot. In (2) we have omitted the superconducting term as irrelevant to our model. We also choose a vertically coupled geometry for our system to minimize the change in charging energy when the electron hops from one dot to another.²⁵ If this energy is smaller than all other relevant scales, then the charging term can be omitted (or absorbed into the chemical potential) since the total number of electrons in the two-dot system remains unchanged.

The (μ, τ) label the basis of the two coupled quantum dots without interaction, that is, it is the set of eigenstates of $H^{(1)} + H^{(2)} + V$. Here μ is the orbital quantum number and τ is a twofold degenerate Kramers index. In this basis the a -th component of total spin reads¹⁸

$$S^a = \sum_{i_0 s s'} c_{i_0 s}^\dagger \frac{\sigma_{ss'}^a}{2} c_{i_0 s'} = \sum_{\mu \tau, \nu \tau'} (M^a)_{\nu \tau'}^{\mu \tau} c_{\mu \tau}^\dagger c_{\nu \tau'}, \tag{3}$$

where i_0 is an Orthogonal basis in the first dot alone (it could be the eigenbasis of $H^{(1)}$ but it does not have to be), and the matrix element M^a is defined as:

$$(M^a)_{\nu \tau'}^{\mu \tau} = \sum_{i_0, s s'} \psi_{\mu \tau}^*(i_0, s) \frac{\sigma_{ss'}^a}{2} \psi_{\nu \tau'}(i_0, s'). \tag{4}$$

We reiterate that the first summation in Eq.(3) and the summation in Eq.(4) is over an Orthogonal basis in the first dot alone, while the second summation in Eq.(3) is over the eigenbasis of the total non-interacting Hamiltonian $H^{(1)} + H^{(2)} + V$. Also, $\sigma_{ss'}^a$ are the Pauli matrices, $\psi_{\mu \tau}(i_0, s)$ is the wave function of the state μ, τ in the first dot.

We use Eq.(2) to calculate the partition function $Z = Tr[\exp(-\beta H)]$, using the imaginary time path integral formalism:

$$Z = Tr(e^{-\beta H}) \Rightarrow Z = \int \prod_{\mu \tau} \mathcal{D}\bar{c}_{\mu \tau} \mathcal{D}c_{\mu \tau} \mathcal{D}\mathbf{h} e^{-\int_0^\beta \mathcal{L} dt}, \tag{5}$$

where the Euclidean Lagrangian is:

$$\mathcal{L} = \frac{|\mathbf{h}|^2}{4J} + \sum_{\mu\tau} \bar{c}_{\mu\tau} (\partial_t + \epsilon_\mu) c_{\mu\tau} - \mathbf{h} \cdot \mathbf{S}. \quad (6)$$

In Eq.(5) we used the Hubbard-Stratonovich transformation to decouple the interaction at the expense of introducing an additional bosonic field \mathbf{h} representing the order parameter. The $c_{\mu\tau}$ and $\bar{c}_{\mu\tau}$ are Grassmann variables.

After switching to the Fourier representation the fermionic fields c, \bar{c} are integrated out. The resulting action for \mathbf{h} is expanded to second order to obtain:

$$S_{eff} \approx \frac{1}{4\beta\delta_1} \sum_{n,a} |h^a(i\omega_n)|^2 \left[\frac{1}{\tilde{J}} - f_n(\beta, E_{X_2}, E_U) \right] \quad (7)$$

$$f_n(\beta, i\omega_n) = -2\delta_1 \sum_{\mu\tau, \nu\tau'} |M^a|^2_{\nu\tau'} \frac{N_F(\epsilon_\mu) - N_F(\epsilon_\nu)}{\epsilon_\mu - \epsilon_\nu - i\omega_n} \quad (8)$$

where $\omega_n = 2\pi n/\beta$, $\tilde{J} = J/\delta_1$ is a dimensionless exchange constant, $N_F(\epsilon_\mu)$ is the Fermi-Dirac occupation of the state μ , and δ_1 is a mean level spacing for the first dot.

Deep into the crossover $E_U, E_{X_2} \gg \delta_1$, we replace $|M^a|^2_{\nu\tau'}$ by its RMT ensemble average. This is justified because in the limit when $\frac{E_{X_2}}{\delta}, \frac{E_U}{\delta} \rightarrow \infty$ the spectral average on a single sample is the same as the ensemble average. The corrections to this vanish in the large- N limit. This is one of the ways in which we use the large- N approximation.

The relevant four wavefunction correlator hidden in $|M^a|^2$ is calculated in Appendix B. We also replace the summation over energy eigenstates by energy integrations. Assuming a constant density of states we obtain

$$f_n(\beta, E_{X_2}, E_U) = \frac{E_U}{E_2^2 - E_1^2} \left[\frac{E_{X_2}^2 + E_{X_2}E_U - E_1^2}{E_1 + |\omega_n|} - \frac{E_{X_2}^2 + E_{X_2}E_U - E_2^2}{E_2 + |\omega_n|} \right] \quad (9)$$

where the interdot tunneling energy scale E_U , the SO crossover energy scale E_{X_2} in the second dot, and the energies $E_{1,2}$ (which are functions of E_U and E_{X_2}) are defined in Appendices B,C.

The instability point is obtained by setting $f_0(\beta, E_{X_2}, E_U) = \tilde{J}^{-1}$. For the coupled-dot system the quantum phase transition takes place at $\tilde{J} = 1$, or $J = \delta_1$, the same result as for one uncoupled dot independent of the crossover energy scales.

We investigate the limit when $E_U \ll E_{X_2}$. In this limit E_U is the only relevant parameter that controls both the coupling between dots and the degree to which spin rotation symmetry

is spoiled in the first dot. In this limit the scaling function becomes $f_n = E_U/(E_U + |\omega_n|)$.

Close to the transition the smallness of $1 - \tilde{J}$ allows us to introduce a new scaling function F_n that describes the interacting system near Stoner transition. The effective action now becomes:

$$S_{eff} = \frac{1}{4\delta_1\beta} \sum_{n,a} |h^a(i\omega_n)|^2 F_n \quad (10)$$

$$F_n = \frac{E_{QCX}}{\tilde{J}E_U} \left(1 + \frac{|\omega_n|}{E_{QCX}}\right) \quad (11)$$

The scaling function F_n in (11) describes how a physical quantity behaves when one goes from the renormalized Fermi liquid to the quantum critical regime. The new characteristic energy scale $E_{QCX} = E_U(1 - \tilde{J})$ can be used to tune the system into the QCR. By changing the single particle parameter E_U in E_{QCX} one can access the QCR governed by interactions.

The Fig. 3 shows the phase diagram in (ω, T) vs. J coordinates. For $J > \delta_1$, the system is in a “bulk” Stoner phase where the magnetization is proportional to the volume of the system. When $J < \delta_1$ and the measurement energy ω satisfies the inequality $E_U \ll \omega < E_T$ one enters an approximate spin-rotation-invariant universal regime described by Universal Hamiltonian H_U . Here the total spin of the system is (approximately) a good quantum number. Lowering the energy to $\omega \sim E_U$ brings us to regime where the system starts seeing spin-orbit coupling and spin fluctuations become important. Below the line $E = E_U(1 - \tilde{J})$ is the renormalized Fermi liquid regime. Above this line, away from the Stoner instability point, is the non-universal regime that depends on many parameters. Close to the instability point $J = \delta_1$ is a Quantum Critical Regime controlled by a single parameter E_{QCX} . One can change the single-particle parameter E_U in E_{QCX} to access the many-body regime.

We proceed to calculate the quasiparticle decay rate near the critical point. Since the particle decays by interacting with quantum fluctuations of collective spin, the decay rate can be obtained from the spin-spin correlation function $\langle S^a(t)S^b(t') \rangle$ which, in turn, can be measured by NMR or EPR. In Fourier space the $S^a S^b$ correlator can be expressed through the bosonic field h^a as follows (see Appendix C for more details)

$$\langle S^a(i\omega_n)S^b(-i\omega_n) \rangle = -\frac{\delta_{ab}}{2J} + \frac{1}{4J^2} \langle h^a(i\omega_n)h^b(-i\omega_n) \rangle. \quad (12)$$

Calculating the $\langle h^a h^b \rangle$ correlator

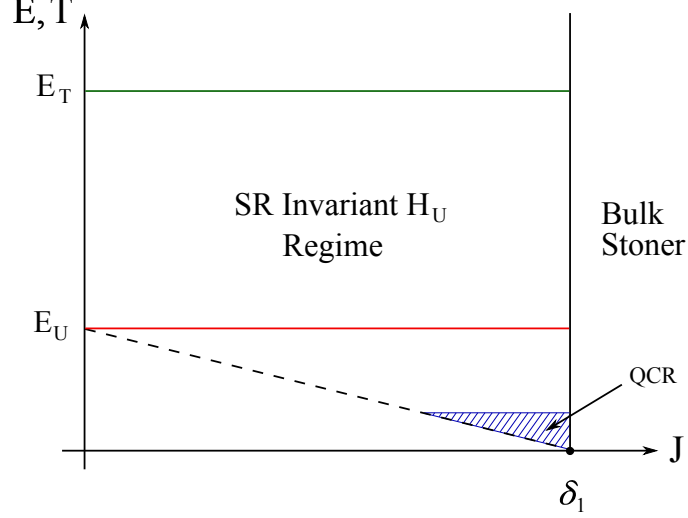


FIG. 3: (Color online) Phase diagram in the E vs. J showing different regimes.

$$\langle h^a(i\omega_n)h^b(-i\omega_n) \rangle = Z^{-1} \int \mathcal{D}\mathbf{h} h^a(i\omega_n)h^b(-i\omega_n) e^{-S_{eff}} = \delta_{ab} \frac{4JE_U}{E_{QCX} \left(1 + \frac{|\omega_n|}{E_{QCX}}\right)} \quad (13)$$

one obtains the following spin-spin correlation function

$$\langle S^a(i\omega_n)S^b(-i\omega_n) \rangle = -\frac{\delta_{ab}}{2J} \left[1 - \frac{2E_U}{E_{QCX} \left(1 + \frac{|\omega_n|}{E_{QCX}}\right)} \right] \quad (14)$$

Switching back to the real time formalism ($i\omega_n \rightarrow \omega + i\eta, \eta \rightarrow 0^+$) in Eq.(14) one obtains the spectral function of spin excitations

$$B(\omega) = -2\Im \left[S^a(\omega)S^b(-\omega) \right] = \delta_{ab} \frac{2E_U}{J} \frac{\omega}{\omega^2 + E_{QCX}^2}. \quad (15)$$

The graph of the spectral function (15) is shown on Fig. 4.

The decay rate of quasiparticles is found by estimating the lowest-order interacting self-energy diagram  with interaction V :

$$V = -\mathbf{h}\mathbf{S} = - \sum_{\mu\tau, \nu\tau'} \mathbf{h}\mathbf{M}_{\nu\tau'}^{\mu\tau} \bar{c}_{\mu\tau} c_{\nu\tau'} \quad (16)$$

The imaginary part of self-energy $\Sigma^{(1)}$ is evaluated to

$$\Im\Sigma^{(1)} = \delta_{ab} \frac{J}{16\pi} \ln \left[\frac{E_{QCX}^2(\epsilon^2 + E_1^2)}{E_1^2(\epsilon^2 + E_{QCX}^2)} \right]. \quad (17)$$

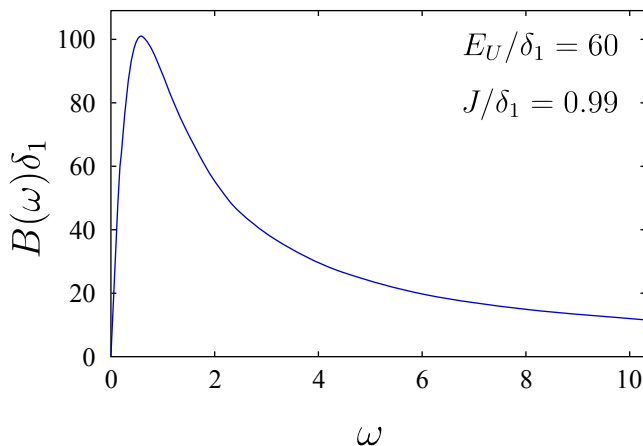


FIG. 4: (Color online) Spectral function for spin-spin excitations.

The decay rate Γ for various regimes is plotted on logarithmic scale in Fig. 5.

III. CONCLUSION

In this paper we have studied a system of two tunnel-coupled quantum dots (small normal metallic grains) near the Stoner transition of the first dot. The first dot has interacting electrons but no spin-orbit coupling, while the other has spin-orbit coupling, but no interactions. The two single-particle crossover energies are E_U , which measures the tunneling strength between the dots, and E_{X_2} which measures the spin-orbit crossover scale in the second dot. Electrons tunneling between the dots carry information about spin-rotation invariance breaking to the first dot, and produce quantum fluctuations of the first dot's spin.

Our focus is on the regime near the Stoner transition when the exchange interaction J is comparable to the mean level spacing δ_1 in the first dot. This regime is characterized by quantum critical fluctuations rising from the interplay between the spin-orbit and interaction parts of the Hamiltonian. For this Quantum Critical Regime we derived the scaling function describing the behavior of system observable near instability point $J = \delta_1$ as a function of the measurement energy ω . The scaling function itself is dependent on a single dimensionless ratio ω/E_{QCX} , as opposed to other parameter regimes where a physical property can depend separately on all the energy scales $E_U, E_{X_2}, \omega, \delta$.

As an illustrative example we compute the scaling form of the quasiparticle decay rate,

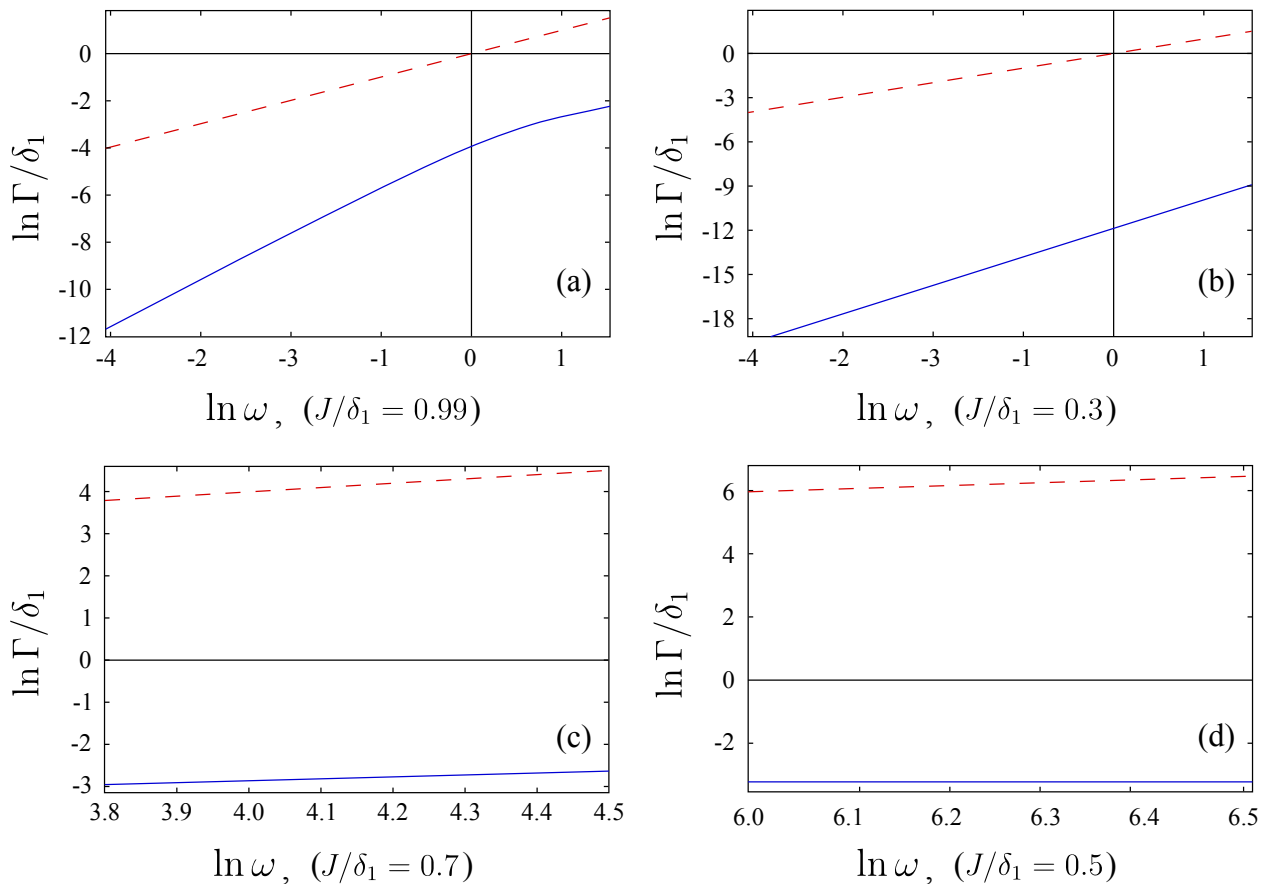


FIG. 5: (Color online) Quasiparticle decay rate (solid line) on a logarithmic scale for different regimes. The dashed line represents $\ln \omega$. Panel (a) shows the decay rate in quantum critical regime. The decay rate in the regime of renormalized Fermi liquid is in panel (b). Panels (c) and (d) show the decay rate in non-universal and Universal regimes respectively.

which can be measured by nonlinear conductance measurements. It has a Fermi liquid-like form for $\omega \ll E_{QCX}$, with the decay rate going as $(\frac{\omega}{E_{QCX}})^2$. However, for $\omega \gg E_{QCX}$ it goes as $\log(\omega/E_{QCX})$.

One of the main conceptual points we wish to make is that there is an intimate relation between the single-particle crossover energies and the many-body quantum critical crossover scale. In the simplest case $E_U \ll E_{X_2}$ this relation is $E_{QCX} = E_U(1 - J/\delta)$. Access to the quantum critical regime can be tuned by changing a single-particle parameter.

An important open question is the effect of quantum criticality on Coulomb Blockade, that is, how are the distributions of the peak positions, heights, and widths affected by quantum criticality. We hope to explore this and other issues in future work.

Acknowledgments

The authors are grateful to the National Science Foundation for partial support under DMR-0703992. GM also wishes to thank the Aspen Center for Physics where some of the work was carried out.

APPENDIX A: GOE TO GSE CROSSOVER IN THE SYSTEM OF TWO COUPLED DOTS

In this appendix we derive one and two particle Green's functions for two coupled dots in crossover between GOE and GSE ensembles. To reduce complexity we consider less general (but relevant to our system) situation when only second dot is in GOE to GSE crossover. The first dot and the hopping bridge belong to GOE ensemble. The generalization where all parts of the system are in crossover can be worked out without difficulty.

The derivation will be rather sketchy for the full derivation in case of GOE to GUE crossover can be found in Ref.^[25].

The Hamiltonian (kinetic part) of two coupled dots is:

$$H = \begin{pmatrix} H_1 & V \\ V^\dagger & H_2 \end{pmatrix}. \quad (\text{A1})$$

where $H_{1,2}$ are the Hamiltonians for dot 1 and 2, V describes coupling between two dots. Following RMT one considers the elements of $H_{1,2}$ and V as Gaussian random variables (quaternions) with zero mean. In the crossover between GOE and GSE Hamiltonians $H_{1,2}$ take the form:

$$H_i = \frac{H_0^i \otimes I + X_i \left[H_x^i \otimes \tau_x + H_y^i \otimes \tau_y + H_z^i \otimes \tau_z \right]}{\sqrt{1 + 3X_i^2}} \quad (\text{A2})$$

Similarly,

$$V = \frac{V^R \otimes I + \Gamma \left[V_x^I \otimes \tau_x + V_y^I \otimes \tau_y + V_z^I \otimes \tau_z \right]}{\sqrt{1 + 3\Gamma^2}} \quad (\text{A3})$$

where H_0^i and H_{xyz}^i are real symmetric and real antisymmetric matrices. V^R and V_{xyz}^I are real and imaginary parts of quantum matrix V (note that elements of V^R and V_{xyz}^I are real numbers). The τ_i matrices are related to Pauli matrices as $\tau_k = i\sigma_k$, $k = x, y, z$.

The X_i and Γ are crossover parameters. The denominators in Eqs. (A2) and (A3) keep mean level spacing constant when X_i and Γ change.

In calculations below we assume $X_1 = \Gamma = 0$, so the first dot and the bridge belong to GOE; the mean level spacing $\delta_1 = \delta_2 \Leftrightarrow N_1 = N_2$.

The elements of H_1 and H_2 are independent random variables with correlations between symmetric and antisymmetric parts

$$\langle H_{mn}^{s,a} H_{st}^{s,a} \rangle = \frac{N_1 \delta_1^2}{\pi^2} (\pm \delta_{mt} \delta_{ns} + \delta_{ms} \delta_{nt}) \quad (\text{A4})$$

where indices s(a) stand for symmetric(antisymmetric); N_1 is the size of matrix H_1 and δ_1 is the mean level spacing (we assume that $N_1 = N_2$, which means $\delta_1 = \delta_2$). Correlation between full matrix elements in crossover is

$$\langle H_{m\xi_m, n\xi_n} H_{s\xi_s, t\xi_t} \rangle = \frac{N_1 \delta_1^2}{\pi^2} \frac{\delta_{mt} \delta_{ns} [(1 - X^2) \delta_{\xi_m \xi_n} \delta_{\xi_s \xi_t} + 2X^2 \delta_{\xi_m \xi_t} \delta_{\xi_n \xi_s}]}{1 + 3X^2} + \frac{N_1 \delta_1^2}{\pi^2} \frac{\delta_{ms} \delta_{nt} [(1 + X^2) \delta_{\xi_m \xi_n} \delta_{\xi_s \xi_t} - 2X^2 \delta_{\xi_m \xi_t} \delta_{\xi_n \xi_s}]}{1 + 3X^2} \quad (\text{A5})$$

Here ξ_i is a "spin" index that numerates elements of τ matrices.

For V matrix correlations between matrix elements are

$$\langle V_{nk'} V_{st'} \rangle = \langle V_{k'n}^\dagger V_{t's}^\dagger \rangle = \langle V_{nk'} V_{t's}^\dagger \rangle = \frac{N_1 \delta_1^2 U}{\pi^2} \delta_{ns} \delta_{k't'} \delta_{\xi_n \xi_{k'}} \delta_{\xi_s \xi_{t'}} \quad (\text{A6})$$

where primed(unprimed) indices belong to the second(first) dot; U is a dimensionless parameter controlling coupling between dots.

One particle Green's function for coupled dots is:

$$G = (E \otimes I - H)^{-1} = \begin{pmatrix} E - H_1 & -V \\ -V^\dagger & E - H_2 \end{pmatrix}^{-1} = \begin{pmatrix} G_{11} & G_{12} \\ G_{21} & G_{22} \end{pmatrix} \quad (\text{A7})$$

Following the steps in Ref.[25] one can obtain the system of Dyson equations for RMT averaged Green's functions G_{11} and G_{22} . In large- N approximation only the rainbow diagrams contribute. In the limit of weak coupling the solution for G_{11} is

$$\langle G_{ab,1}^R \rangle^{-1} = \delta_{ab} \delta_{\xi_a \xi_b} \frac{N_1 \delta_1}{\pi} \left[\epsilon + i\sqrt{1 - \epsilon^2} \right] \left[1 + \frac{U}{2} \left(1 + i\frac{\epsilon}{\sqrt{1 - \epsilon^2}} \right) \right] \quad (\text{A8})$$

where dimensionless energy $\epsilon = \frac{\pi E}{2N_1\delta_1}$.

The two particle Green's function in the first dot can be found from the system of Bethe-Salpeter equations.²⁵ This system describes contribution of ladder and absolutely crossed diagrams.

Expression for the full two particle Green's function is

$$\langle G_{1,ab}^R(E)G_{1,cd}^A(E+\omega) \rangle = D_1 + C_1 \quad (\text{A9})$$

Contribution of ladder diagrams D_1 is

$$D_1 = \delta_{ad}\delta_{bc} \frac{2\pi}{N_1^2\delta_1} \frac{1}{-i\omega} \left[\delta_{\xi_a\xi_b}\delta_{\xi_c\xi_d} \frac{1 + i\frac{E_{X_2}+E_U}{\omega}}{\left(1 + i\frac{E_U}{\omega}\right)\left(1 + i\frac{E_{X_2}+E_U}{\omega}\right) + \frac{E_U^2}{\omega^2}} + \delta_{\xi_a\xi_d}\delta_{\xi_b\xi_c} \frac{-\frac{i}{2}\frac{E_{X_2}E_U^2}{\omega^3}}{\left[\left(1 + i\frac{E_U}{\omega}\right)\left(1 + i\frac{E_{X_2}+E_U}{\omega}\right) + \frac{E_U^2}{\omega^2}\right] \left[\left(1 + i\frac{E_U}{\omega}\right)^2 + \frac{E_U^2}{\omega^2}\right]} \right] \quad (\text{A10})$$

Contribution of absolutely crossed diagrams is

$$C_1 = \delta_{ac}\delta_{bd} \frac{2\pi}{N_1^2\delta_1} \frac{1}{-i\omega} \left[\delta_{\xi_a\xi_b}\delta_{\xi_c\xi_d} \frac{\Pi_{11}^+ + \Pi_{11}^-}{2} + \delta_{\xi_a\xi_d}\delta_{\xi_b\xi_c} \frac{\Pi_{11}^+ - \Pi_{11}^-}{2} \right], \quad (\text{A11})$$

where

$$\Pi_{11}^+ = \frac{1 + i\frac{E_{X_2}+E_U}{\omega}}{\left(1 + i\frac{E_U}{\omega}\right)\left(1 + i\frac{E_{X_2}+E_U}{\omega}\right) + \frac{E_U^2}{\omega^2}}$$

$$\Pi_{11}^- = \frac{1 + i\frac{E_U}{\omega}}{\left(1 + i\frac{E_U}{\omega}\right)^2 + \frac{E_U^2}{\omega^2}}$$

Crossover energy scales E_{X_2} and E_U are defined as $E_{X_2} = 8X_2^2N_1\delta_1/\pi$ and $E_U = 2UN_1\delta_1/\pi$.

APPENDIX B: CORRELATION OF FOUR WAVE FUNCTIONS

Consider the matrix element average $\langle |M^a|^2 \rangle$. More generally,

$$\langle M_{m\tau,m'\tau'}^a M_{m'\tau',m\tau}^b \rangle = \sum_{iss',i_1s_1s'_1} \frac{\sigma_{ss'}^a}{2} \frac{\sigma_{s_1s'_1}^b}{2} \langle \psi_{m\tau}^*(i,s) \psi_{m'\tau'}(i,s') \psi_{m'\tau'}^*(i_1,s_1) \psi_{m\tau}(i_1,s'_1) \rangle. \quad (\text{B1})$$

where (i, s) is the basis of first uncoupled dot, and (m, τ) is the basis of two coupled dots without interaction; $\psi_{m\tau}(is)$ is the wave function of electron in the first dot in (m, τ) basis.

In full analogy with derivations in Ref.[²⁵] for GOE to GSE crossover one gets the following expression for four wave function correlator

$$\langle \psi_{n\tau_n}(\alpha)\psi_{n\tau_n}^*(\beta)\psi_{m\tau_m}(\gamma)\psi_{m\tau_m}^*(\nu) \rangle = \frac{\delta^2}{8\pi^2} [\delta_{\alpha\nu}\delta_{\beta\gamma}\Re[D_1] + \delta_{\alpha\gamma}\delta_{\beta\nu}\Re[C_1]] \quad (\text{B2})$$

where $\Re[D_1]$ and $\Re[C_1]$ are real parts of diffuson and Cooperon contributions to the two particle Green's function. Mean level spacing δ of coupled dot system is $\delta = \delta_1/2$.

Comparing indices in Eqs. (B1) and (B2) after summation over i and i' it is easy to see that the diffuson contribution is N_1^2 times larger than that of Cooperon. Therefore, the Cooperon contribution is ignored in large- N approximation.

Substituting (B2) into (B1) and using results of Appendix A for $\Re[D_1]$ one obtains

$$\langle M_{m\tau, m'\tau'}^a M_{m'\tau', m\tau}^b \rangle = \delta_{ab} \frac{\delta_1}{32\pi} \frac{E_U}{E_2^2 - E_1^2} \left[\frac{E_{X_2}^2 + E_{X_2}E_U - E_1^2}{\omega^2 + E_1^2} - \frac{E_{X_2}^2 + E_{X_2}E_U - E_2^2}{\omega^2 + E_2^2} \right] \quad (\text{B3})$$

Here E_U and E_{X_2} are the crossover energy scales defined in Appendix A. Energy scales $E_{1,2}$ are equal to $E_{1,2} = a_{1,2}E_{X_2}$, where

$$a_{1,2}^2 = \frac{4b^2 + 2b + 1 \pm \sqrt{(4b^2 + 2b + 1)^2 - 4b^2}}{2}$$

with b defined as $b = E_U/E_{X_2}$.

APPENDIX C: SPIN-SPIN CORRELATOR

The spin-spin correlator (spin Green's function) is defined by:

$$\langle S^a(t)S^b(t') \rangle = Z^{-1} \int \mathcal{D}\mathbf{h}\mathcal{D}\bar{\eta}\mathcal{D}\eta S^a(t)S^b(t')e^{-S} \quad (\text{C1})$$

where $S^a(t)$ is a component of total spin of the system. Let's split the action S (defined by Eq. (6)) in two parts $S = S_1 + S_2$. Here S_1 is the part of the action containing spin S^a , $S_1 = -\int dt h^a S^a(t)$, and $S_2 = S - S_1$ contains everything else.

Then spin-spin correlator can be written as

$$\langle S^a(t)S^b(t') \rangle = Z^{-1} \int \mathcal{D}\mathbf{h}\mathcal{D}\bar{\eta}\mathcal{D}\eta \left[\frac{\partial}{\partial h^a(t)} \frac{\partial}{\partial h^b(t')} e^{-S_1} \right] e^{-S_2}. \quad (\text{C2})$$

Integration by parts in Eq. (C2) transfers functional derivative on $\exp(-S_2)$ term. Performing differentiation one obtains relation

$$\langle S^a(t)S^b(t') \rangle = -\frac{\delta(t-t')}{2J} \delta_{ab} + \frac{1}{4J^2} \langle h^a(t)h^b(t') \rangle \quad (\text{C3})$$

In Fourier space relation (C3) reads

$$\langle S^a(i\omega_n)S^b(-i\omega_n) \rangle = -\frac{\delta_{ab}}{2J} + \frac{1}{4J^2} \langle h^a(i\omega_n)h^b(-i\omega_n) \rangle \quad (\text{C4})$$

APPENDIX D: QUASIPARTICLE DECAY RATE

The interacting self-energy of electron  in Matsubara formalism is evaluated to

$$\begin{aligned} \Sigma^{(1)} &= -\beta^{-1} \sum_{\omega_n, \gamma} \mathcal{G}_0(ip_n - i\omega_n) \mathcal{D}_0(i\omega_n) \langle |M_{\alpha\gamma}|^2 \rangle \\ &= -\beta^{-1} \sum_{\gamma} \langle |M_{\alpha\gamma}|^2 \rangle \sum_{\omega_n} \iint_{-\infty}^{\infty} \frac{d\omega' d\omega''}{(2\pi)^2} \frac{A_{\gamma}(\omega')}{ip_n - i\omega_n - \omega'} \frac{H(\omega'')}{i\omega_n - \omega''}, \end{aligned} \quad (\text{D1})$$

where \mathcal{G}_0 and \mathcal{D}_0 are non-interacting Green's functions for electron and bosonic excitation and $A(\omega')$ and $H(\omega'')$ are their spectral representations; $\omega_n = 2n\pi/\beta$ and $p_n = (2n+1)\pi/\beta$ are even and odd Matsubara frequencies.

After summation over ω_n imaginary part of self energy reads

$$\Im[\Sigma^{(1)}] = -\frac{1}{2\delta_1} \int_0^{\omega} \langle |M_{\alpha\omega'}|^2 \rangle H(\omega - \omega') d\omega'. \quad (\text{D2})$$

Here we employed the non-interacting expression for electron spectral function $A_{\gamma}(\omega') = 2\pi\delta(\omega' - E_{\gamma})$ assuming small broadening of energy levels. Spectral function $H(\omega)$ for bosonic excitations is

$$H(\omega) = -2\Im \left[\langle h^a(\omega)h^a(-\omega) \rangle \right] = 8JE_U \frac{\omega}{\omega^2 + E_{QCX}^2}. \quad (\text{D3})$$

Using Eqs. (B3) and (D3) we finally obtain the decay rate near the pole

$$\Im[\Sigma^{(1)}] = -\Gamma/2 = \delta_{ab} \frac{J}{16\pi} \frac{E_U^2}{E_2^2 - E_1^2} \left[\frac{E_{X_2}^2 + E_{X_2}E_U - E_1^2}{E_1^2 - E_{QCX}^2} \ln \frac{E_{QCX}^2(\omega^2 + E_1^2)}{E_1^2(\omega^2 + E_{QCX}^2)} - \frac{E_{X_2}^2 + E_{X_2}E_U - E_2^2}{E_2^2 - E_{QCX}^2} \ln \frac{E_{QCX}^2(\omega^2 + E_2^2)}{E_2^2(\omega^2 + E_{QCX}^2)} \right]. \quad (\text{D4})$$

* Electronic address: zelyak@pa.uky.edu

† Electronic address: murthy@pa.uky.edu

- ¹ E. Akkermans and G. Montambaux, *Mesoscopic Physics of Electrons and Photons* (Cambridge University Press, 2007).
- ² G. Dresselhaus, Phys. Rev. **100**, 580 (1955).
- ³ Y. Bychkov and E. Rashba, JETP Lett. **39**, 78 (1984).
- ⁴ M. L. Mehta, *Random Matrices* (Academic Press, 2004).
- ⁵ H.-J. Stöckmann, *Quantum Chaos: An Introduction* (Cambridge University Press, 1999).
- ⁶ P. W. Brouwer, J. N. H. J. Cremers, and B. I. Halperin, Phys. Rev. B **65**, 081302(R) (2002).
- ⁷ D. A. Gorokhov and P. W. Brouwer, Physical Review B (Condensed Matter and Materials Physics) **69**, 155417 (pages 14) (2004).
- ⁸ Y. Oreg, P. W. Brouwer, X. Waintal, and B. I. Halperin, <http://arxiv.org/abs/cond-mat/0109541> (2001).
- ⁹ G. Murthy and R. Shankar, Physical Review B (Condensed Matter and Materials Physics) **75**, 075327 (pages 12) (2007).
- ¹⁰ S. Adam, P. W. Brouwer, J. P. Sethna, and X. Waintal, Phys. Rev. B **66**, 165310 (2002).
- ¹¹ A. V. Andreev and A. Kamenev, Phys. Rev. Lett. **81**, 3199 (1998).
- ¹² P. W. Brouwer, Y. Oreg, and B. I. Halperin, Phys. Rev. B **60**, R13977 (1999).
- ¹³ H. U. Baranger, D. Ullmo, and L. I. Glazman, Phys. Rev. B **61**, R2425 (2000).
- ¹⁴ I. L. Kurland, I. L. Aleiner, and B. L. Altshuler, Phys. Rev. B **62**, 14886 (2000).
- ¹⁵ G. Murthy and H. Mathur, Phys. Rev. Lett. **89**, 126804 (2002).
- ¹⁶ G. Murthy and R. Shankar, Phys. Rev. Lett. **90**, 066801 (2003).
- ¹⁷ G. Murthy, R. Shankar, D. Herman, and H. Mathur, Physical Review B (Condensed Matter and Materials Physics) **69**, 075321 (pages 33) (2004).

- ¹⁸ Y. Alhassid and T. Rupp, cond-mat/0312691 (2003).
- ¹⁹ G. Murthy, Physical Review B (Condensed Matter and Materials Physics) **70**, 153304 (pages 4) (2004).
- ²⁰ S. Sachdev, *Quantum Phase Transitions* (Cambridge University Press, 2001).
- ²¹ B. L. Altshuler, Y. Gefen, A. Kamenev, and L. S. Levitov, Phys. Rev. Lett. **78**, 2803 (1997).
- ²² U. Sivan, Y. Imry, and A. Aronov, Europhys. Lett. **28**, 115 (1994).
- ²³ K. Efetov, *Supersymmetry in Disorder and Chaos* (Cambridge University Press, 1999).
- ²⁴ S. Adam, P. W. Brouwer, and P. Sharma, Phys. Rev. B **68**, 241311(R) (2003).
- ²⁵ O. Zelyak, G. Murthy, and I. Rozhkov, Physical Review B (Condensed Matter and Materials Physics) **76**, 125314 (pages 26) (2007).